A DFT study on the behavior of NO$_2$ in the selective catalytic reduction of nitric oxides with ammonia on a V$_2$O$_5$ catalyst surface

Xiang Gao*, Xue-sen Du, Ye Jiang, Yang Zhang, Zhong-yang Luo, Ke-fa Cen

State Key Laboratory of Clean Energy Utilization, Zhejiang University, Zheda Road 38, Hangzhou 310027, PR China

ARTICLE INFO

ABSTRACT

DFT calculations were carried out to study the behavior of NO$_2$ in the selective catalytic reduction of nitric oxides with ammonia on the surface of the V$_2$O$_5$ catalyst. The results showed that NO$_2$ could readily reoxidize V^{4+}–OH through two reaction routes: (1) NO$_2$ directly reoxidizing V^{4+}–OH to V^{5+}=O and (2) NO$_2$ reacting with H$_2$O or NH$_3$ to produce HNO$_3$, which subsequently reoxidizes V^{4+}–OH to V^{5+}=O. The rate-determining step of route 1 is the desorption of *cis*-HNO$_2$ from the reoxidized V^{5+}=O, being endothermic by 9.91 kcal/mol. Route 2 possesses an energy barrier of 7.44 kcal/mol, less than route 1. This energetic comparison shows that route 2 is the predominant reaction mechanism at low temperature. Reactions of the by-product, HNO$_2$, were also investigated. The results showed that both *cis*-HNO$_2$ (route 1) and *trans*-HNO$_2$ (route 2) can either react with NH$_3$, producing H$_2$O and N$_2$, or react with themselves, producing H$_2$O, NO and NO$_2$. A systemic description of the behavior for NO$_2$ in "fast" SCR on V$_2$O$_5$ surface, including the reaction routes and energy profiles, has been proposed in our work.

1. Introduction

Selective catalytic reduction (SCR) with NH$_3$ is thought to be state-of-the-art technology for the abatement of NO$_x$ emitted from stationary sources and vehicles [1,2]. Numerous experimental and theoretical studies have been carried out to reveal the SCR reaction mechanism over V$_2$O$_5$ catalysts [3–5]. The stoichiometry of the traditional SCR, known as the "standard" SCR, is given in Eq. (1):

$$4NH_3 + 4NO + O_2 \rightarrow 4N_2 + 6H_2O \tag{1}$$
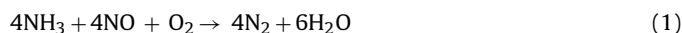
Nevertheless, the current method of SCR over a V$_2$O$_5$ catalyst requires a high operation temperature (300–400 °C), which cannot be achieved in diesel engines and the low-temperature regions of stationary plants. One promising solution to this problem is represented by the "fast" SCR with stoichiometry:

$$2NH_3 + NO + NO_2 \rightarrow 2N_2 + 3H_2O \tag{2}$$
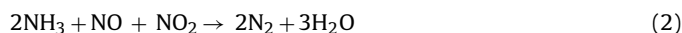
The promotional effect of NO$_2$ on the SCR reaction was first observed in 1981, when Kato et al. [6] reported that the reaction involving equimolar quantities of NO and NO$_2$ feed mixture (Eq. (2)) showed a considerably higher reaction rate than the "standard" SCR (Eq. (1)) at low temperatures. Thereafter, numerous authors [7–19] have dedicated themselves to the work of revealing the mechanism

of the "fast" SCR. Koebel et al. [7–10] have done significant work in this field, including giving the definition of "fast" SCR in 2001. They found that the "fast" SCR reaction exhibits a reaction rate at least 10 times higher than that of the well-known "standard" SCR reaction with pure NO. The reoxidation of V^{4+}–OH by NO$_2$, O$_2$ in "standard" SCR, may be the main reason for enhancing the reaction rate of the "fast" SCR, according to their experimental results. They also pointed out that NH$_4$NO$_3$ will deposit on the catalyst surface at temperatures below 140 °C. Nova et al. [11,12,14–16,18,20] have also done outstanding work in order to illuminate the mechanism of the "fast" SCR. They proposed a novel mechanism involving the formation of "ammonium nitrate" as an intermediate and its subsequent reaction with NO as the rate-determining step. The behavior of vanadium sites in the "ammonium nitrate" route has been well discussed by Tronconi et al. [13], who reported that reduced V^{4+}–OH is not active in the SCR reaction. He also pointed out that both NO$_2$ and HNO$_3$ could reoxidize V^{4+}–OH to V^{5+}=O at lower temperatures than O$_2$ ("standard" SCR). The stoichiometry for the reaction of ammonium nitrate is shown in Eq. (3):

$$NH_4NO_3 + NO \rightarrow NO_2 + N_2 + H_2O \tag{3}$$
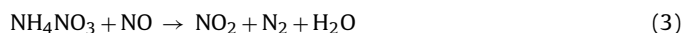
This reaction involves the decomposition of ammonium nitrate to HNO$_3$ and NH$_3$ and the redox of vanadium sites, as reported by several authors [11,12,16]. Li and Li performed a DFT study of the "fast" SCR over Fe-exchanged zeolites [21]. The result showed a significant promotional effect of NO$_2$ on the SCR reaction.

Although the behavior of NO$_2$ in the SCR reaction on V$_2$O$_5$ surface has been studied in numerous experiments, the delicate

---

reaction mechanism and energy profile have rarely been involved. Based on previous work, the behavior of NO_2 in the SCR reaction on the V_2O_5 surface could follow two reaction routes: (1) NO_2 directly reoxidizing V^{4+}–OH to V^{5+}=O and (2) NO_2 reacting with H_2O to produce HNO_3, which subsequently reoxidizes V^{4+}–OH to V^{5+}=O. The objective of the present study is to elucidate the full sequence of reaction steps including intermediates and transition state geometries, and the energetics of these two reaction routes. A systematic description of the behavior of NO_2 in the "fast" SCR is proposed.

2. Calculation details

All density functional theory (DFT) calculations were performed with Gaussian 03 [22] code using the gradient corrected Becke's [23,24] three-parameter hybrid exchange functional in combination with the correlation functional of Lee et al. [25] (B3LYP). The 6-31G(d,p) basis set was employed for all atoms. Each stationary structure has been confirmed as a minimum-energy structure or a transition state from the calculated vibrational frequencies. A geometry with no imaginary frequency (negative sign) indicates a minimum-energy structure, while a geometry with only one imaginary frequency implies a transition state. Zero point correction and vibrational frequencies obtained by frequency calculations were scaled by 0.9607 [26].

A model cluster ($V_2O_9H_{10}$) including two adjacent vanadium (V^{4+}–OH) sites was used to represent the reduced V_2O_5 catalyst surface in this DFT study, as shown in Fig. 1. This model cluster has been successfully used in numerous publications [5,27–30]. The reduced V^{4+}–OH sites are produced after the reaction of NH_3 and NO on the V^{5+}=O sites [13]. To be in accordance with the real electronic environment of the periodic structure on the V_2O_5 catalyst surface, only the atoms in the dashed lines (Fig. 1) were relaxed, while the others were kept fixed in all the optimization processes. The coordinates and bond lengths of the fixed atoms are referred to in previous publications [5,30–35]. Frequency calculations were carried out to identify the applicability of the model cluster. The calculated frequency of the hydroxyl stretching for V^{4+}–OH is 3680 cm^{-1}, in good agreement with the value 3655 cm^{-1} measured by IR experiments on a reduced titania-supported vanadia catalyst [36]. This
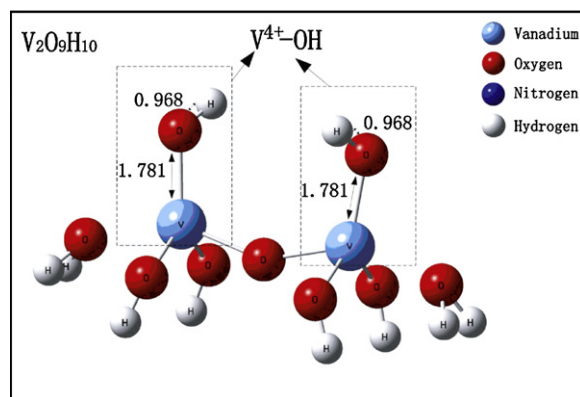

Fig. 1. Optimized structure of the model cluster for the reduced V_2O_5 catalyst. Bond lengths are in Å.

suggests a good agreement between this model cluster and the real catalyst.

3. Results and discussion

3.1. Direct reoxidization of V^{4+}–OH by NO_2

3.1.1. The adsorption and reaction of NO_2 on V^{4+}–OH

NO_2 can readily reoxidize the V^{4+}–OH sites, as pointed out by Koebel et al. [7–9], with the production of V^{5+}=O and cis-HNO_2 (Fig. 2). The stoichiometry is shown in the following equation:

$$V^{4+}\text{–OH} + NO_2 \rightarrow V^{5+}\text{=O} + cis\text{-}HNO_2 \qquad (4)$$
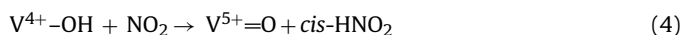
As can be seen from Figs. 2 and 3, NO_2 is first adsorbed on to the cluster ($V_2O_9H_{10}$), an exothermic process, releasing 52.39 kcal/mol. Then the hydrogen of the V^{4+}–OH will be captured by the adsorbed NO_2, producing an adsorbed HNO_2 on the cluster ($V_2O_9H_9$–HNO_2, as shown in Fig. 2). This step releases an energy of 5.15 kcal/mol. Afterwards, with an activation energy of 9.91 kcal/mol, the cis-HNO_2 desorbs from the cluster, accomplishing the reoxidization of V^{4+}–OH to V^{5+}=O ($V_2O_9H_9$ in Fig. 2). The $V_2O_9H_9$ includes a

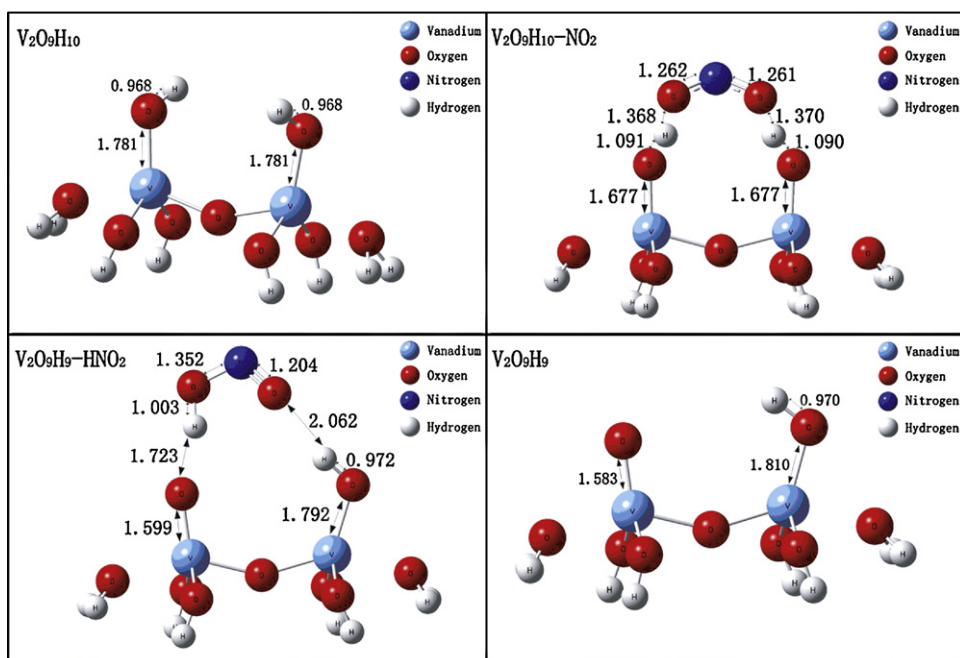**Fig. 2.** Optimized structures of all the stationary points in the direct reoxidization of V^{4+}–OH by NO_2. Bond lengths are in Å.
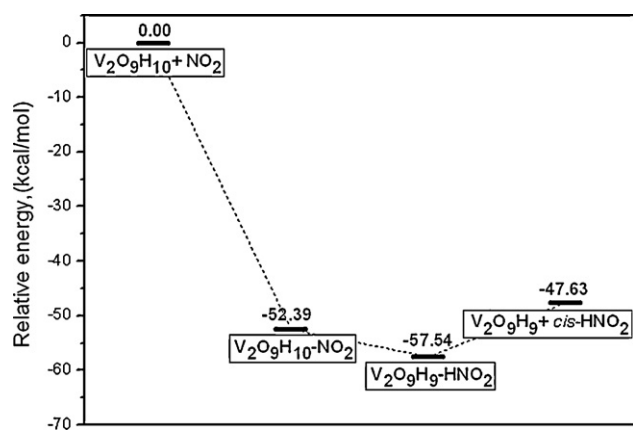
Fig. 3. Energy profile for direct reoxidization of V^{4+}–OH by NO_2 (relative to $V_2O_9H_{10} + NO_2$).

V^{5+}=O and a V^{4+}–OH, which can be further oxidized by NO_2 or other species.

Frequency calculations for $V_2O_9H_{10}$–NO_2 were carried out to compare with the experimental results of Dines et al. [36]. This comparison shows excellent agreement between the frequencies 1585, 1202 and 1620, 1225 cm^{-1} for the calculated and experimental results, respectively. The calculation shows that the hydroxyl of HNO_2 in $V_2O_9H_9$–HNO_2 possesses a swinging frequency at 1349 cm^{-1}, while the experimental result [37] turns out to be 1218 cm^{-1}. The difference between calculation and experiment may be attributed to the fact that the adsorption of HNO_2 on a real catalyst surface will be influenced by the support. The V^{5+}=O has a stretching frequency at 1062 cm^{-1}, according to the frequency calculation for $V_2O_9H_9$, in excellent agreement with the experimental result [37] of 1032 cm^{-1}.

3.1.2. Reaction of the by-product cis-HNO₂

The reactions of cis-HNO_2 are discussed in this subsection. Savara et al. [17] found that NH_4NO_2 could readily decompose at the temperatures less than 100 °C to N_2 and H_2O. In our work, quantum chemistry calculations were carried out to reveal the reaction of HNO_2 and NH_3. The products of the reaction between HNO_2 and

NH_3 were H_2O and nitrosamide (H_2NNO), which is thought to be the key intermediate in the SCR reaction [5]. H_2NNO could further transform and decompose on V_2O_5 catalyst surface to N_2 and H_2O, the desired end products. The reaction between HNO_2 and NH_3 could be described as the following equation (Eq. (5)):

$$cis\text{-}HNO_2 + NH_3 \rightarrow H_2NNO + H_2O \tag{5}$$
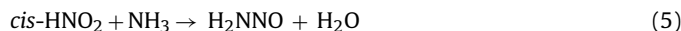
The reaction between cis-HNO_2 and NH_3 on the catalyst surface has two types, i.e. reaction of adsorbed NH_3 with gaseous cis-HNO_2 and reaction of adsorbed cis-HNO_2 with gaseous NH_3. As can be seen from Fig. 4, reaction of adsorbed NH_3 with gaseous cis-HNO_2 (A1–A5) starts with the NH_3 adsorption on the catalyst surface with an exothermic energy of 12.85 kcal/mol. Gaseous cis-HNO_2 will further react with the adsorbed NH_3 to produce adsorbed H_2NNO–H_2O (A4, both H_2O and H_2NNO are adsorbed on the catalyst surface) via a transition state (A3), costing an activation energy of 29.98 kcal/mol. In A3, a hydrogen of the adsorbed NH_3 is being transferred to one oxygen of the cis-HNO_2, simultaneously a N–N bond between NH_3 and HNO_2 is being formed. Given an endothermic energy of 25.20 kcal/mol, both H_2O and H_2NNO could desorb from the catalyst surface. H_2NNO will re-adsorb on active site to produce N_2 and H_2O.

Reaction of adsorbed cis-HNO_2 with gaseous NH_3 (B1–B5) starts with the cis-HNO_2 adsorption on the catalyst surface with an exothermic energy of 9.11 kcal/mol. The adsorbed cis-HNO_2 will react with gaseous NH_3 via a transition state (B3) with an activation energy of 25.99 kcal/mol. Desorption of the products, H_2O and H_2NNO will be endothermic by 18.40 kcal/mol.

The reaction between two cis-HNO_2 has been studied by Mebel et al. [38]. In our present work, this reaction was calculated to compare with the reaction between HNO_2 and NH_3, aiming at revealing the real behavior of the by-product cis-HNO_2. According to Eq. (6), cis-HNO_2 would react with each other to produce H_2O, NO and NO_2:

$$cis\text{-}HNO_2 + cis\text{-}HNO_2 \rightarrow NO_2 + NO + H_2O \tag{6}$$

Cis-HNO_2 can be readily adsorbed onto the catalyst surface. Thus Eq. (6) will happen between adsorbed HNO_2 and gaseous HNO_2. The energy profile of this reaction is shown in Fig. 4 (C1–C5). Adsorbed HNO_2 and gaseous HNO_2 will react to produce adsorbed H_2O–NO–NO_2 (C4, H_2O, NO and NO_2 adsorbed on the catalyst surface) via a transition state (C3). In C4, a hydrogen of
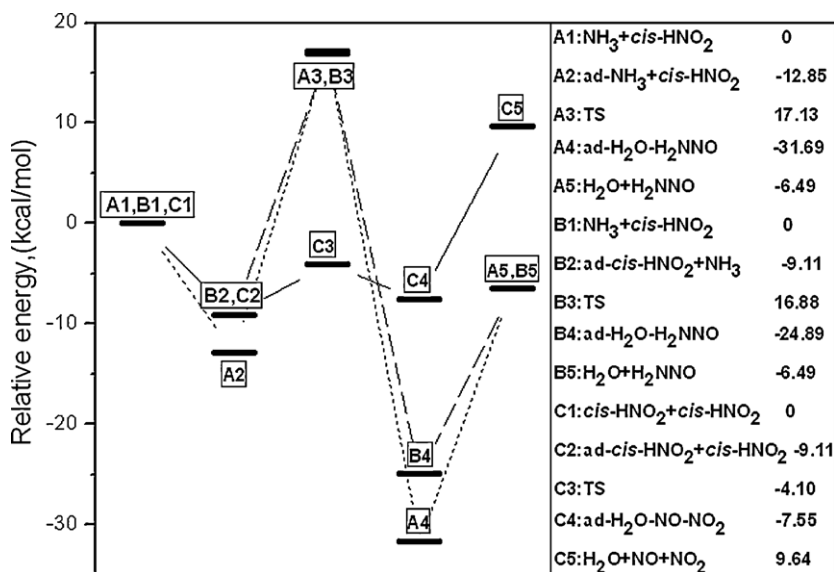

Fig. 4. Energy profile for the reaction between adsorbed NH_3 and gaseous HNO_2 (A1–A5, relative to NH_3 + cis-HNO_2); adsorbed HNO_2 and gaseous NH_3 (B1–B5, relative to NH_3 + cis-HNO_2), adsorbed cis-HNO_2 and gaseous cis-HNO_2 (C1–C5, relative to cis-HNO_2 + cis-HNO_2). 'ad-' indicates the adsorbed species on the catalyst surface. The values (given in kcal/mol) on the right side of this figure are the corresponding relative energies.
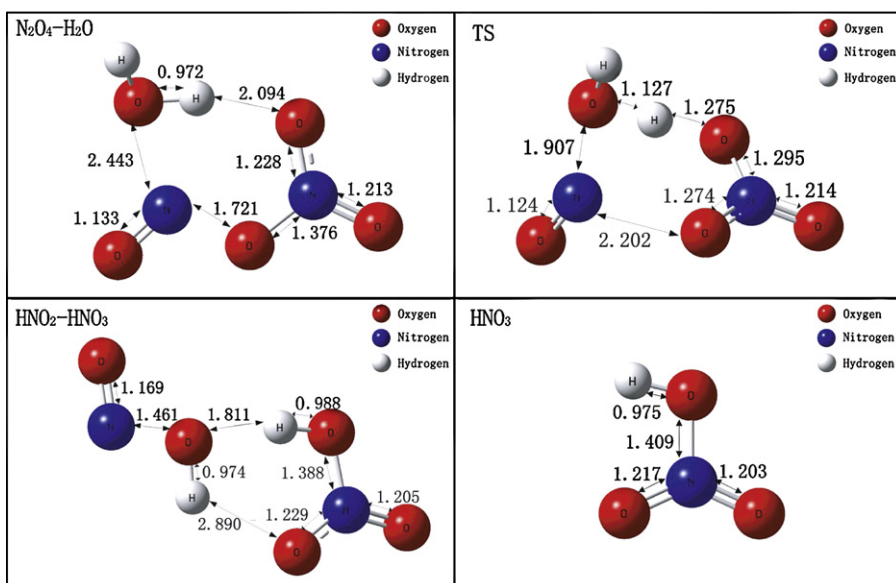
Fig. 5. Optimized structures of all the stationary points in the reaction of NO_2 with H_2O. Bond lengths are in Å.

gaseous cis-HNO_2 is being transferred to the hydroxy oxygen of a adsorbed cis-HNO_2. This process would cost an activation energy of 5.01 kcal/mol and has an exothermic energy of 3.45 kcal/mol. H_2O, NO and NO_2 will desorb from the catalyst surface, being endothermic by 17.01 kcal/mol.

In summary, cis-HNO_2 could either react with NH_3 or cis-HNO_2. The reaction of adsorbed NH_3 with gaseous cis-HNO_2 and adsorbed cis-HNO_2 with gaseous NH_3 will cost a barrier energy of 29.98 and 25.99 kcal/mol, respectively. Nevertheless, the reaction between two cis-HNO_2 (Eq. (6)) just has a barrier energy of 18.40 kcal/mol. Thus, the by-product cis-HNO_2 prefers the reaction of two cis-HNO_2 to produce H_2O, NO and NO_2 in low temperature. This result shows a good agreement with the work of Koebel et al. [9], which revealed that the reoxidization of V^{4+}–OH by NO_2 would produce H_2O and NO.

3.2. Reoxidization of V^{4+}–OH by HNO_3 (produced by the reaction of NO_2 with H_2O or NH_3)

3.2.1. Reaction of NO_2 with H_2O and NH_3

HNO_3 acting as an intermediate to reoxidize V^{4+}–OH has been published by several authors [11–16]. As known for a long time, NO_2 can readily react with H_2O with a production of $trans$-HNO_2 and HNO_3. The stoichiometry is given in the following equation:

$$2NO_2 + H_2O \rightarrow trans\text{-}HNO_2 + HNO_3 \tag{7}$$

In this subsection, DFT calculation was performed to study the reaction route of Eq. (7) (Figs. 5 and 6). This reaction starts from the combination of H_2O and two NO_2 (N_2O_4–H_2O in Fig. 5), producing an exothermic energy of 6.58 kcal/mol. N_2O_4–H_2O further converts to HNO_2–HNO_3 via a transition state (TS), costing an activation energy of 2.53 kcal/mol. This transforming process yields an exothermic energy of 7.39 kcal/mol. Afterwards, HNO_2–HNO_3 decomposes to $trans$-HNO_2 and HNO_3 (Fig. 5) accompanying with an endothermic energy of 7.13 kcal/mol. The energy profile indicates that decomposition of HNO_2–HNO_3 to $trans$-HNO_2 and HNO_3 is the control step of the reaction between NO_2 and H_2O.

The reaction between NO_2 and NH_3 has also been largely reported by several authors [11,13,15]. NO_2 can react with NH_3 at low temperature to produce NH_4NO_3, N_2 and H_2O, as shown in Eq. (8). NH_4NO_3 can readily decompose to NH_3 and HNO_3 at the SCR temperature:

$$2NO_2 + 2NH_3 \rightarrow H_2O + N_2 + NH_4NO_3 \tag{8}$$

The reaction route and energy profile of reaction between NO_2 and NH_3 are shown in Figs. 7 and 8, respectively. In the transition state (TS) of Fig. 7, a hydrogen of NH_3 is being transferred to the oxygen of NO_2 and a N–N bond is being formed. The activation energy is only 2.34 kcal/mol. The largest energy barrier of this reaction is 4.12 kcal/mol, consumed by the decomposition of H_2NNO–HNO_3. H_2NNO will further transform to H_2O and N_2, and HNO_3 can readily combine with NH_3 to produce NH_4NO_3, thus this calculation is accordant with Eq. (8). Low barrier energy confirms the results found by other authors [11,13,15].

3.2.2. Reoxidation of V^{4+}–OH by HNO_3

HNO_3 (one of the products in reactions (7) and (8)) is a strong oxidizing agent and can easily reoxidize V^{4+}–OH to V^{5+}=O, following Eqs. (9) and (10):
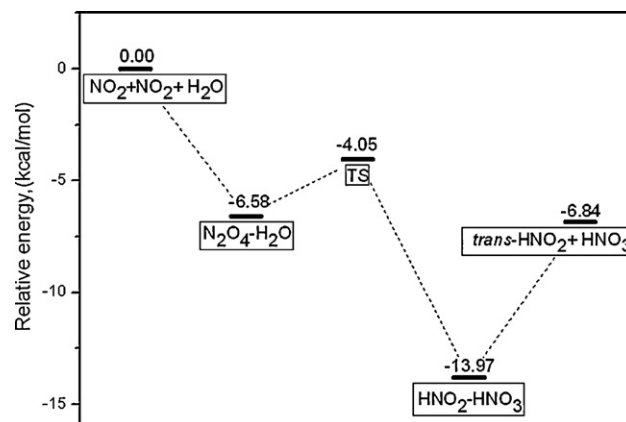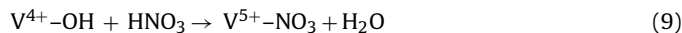
$$V^{4+}\text{–}OH + HNO_3 \rightarrow V^{5+}\text{–}NO_3 + H_2O \tag{9}$$

$$V^{5+}\text{–}NO_3 \rightarrow V^{5+}\text{=}O + NO_2 \tag{10}$$

Fig. 6. Energy profile for the reaction between NO_2 and H_2O (relative to $NO_2 + NO_2 + H_2O$).
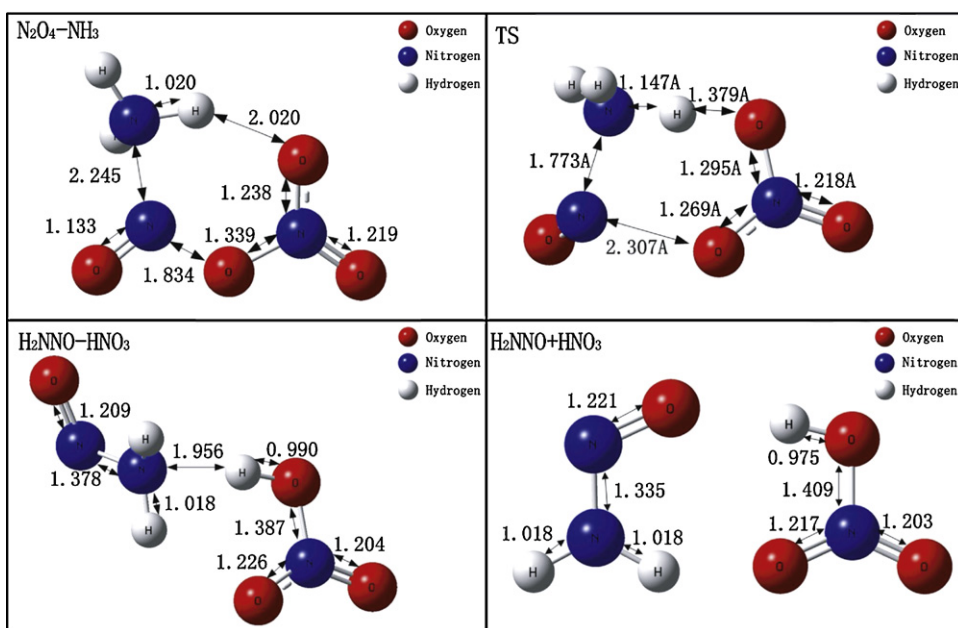
Fig. 7. Optimized structures of all the stationary points in the reaction of NO_2 with NH_3. Bond lengths are in Å.

Fig. 9 exhibits the optimized structures in the reoxidation process by HNO_3. The energy in Fig. 10 is given relative to the total energy of $V_2O_9H_{10} + HNO_3$. Initially, HNO_3 is adsorbed on to the $V_2O_9H_{10}$ cluster ($V_2O_9H_{10}–HNO_3$), releasing an energy of 14.28 kcal/mol. Then, $V_2O_9H_{10}–HNO_3$ is transformed to a $V_2O_8H_9–NO_3–H_2O$ cluster in which H_2O is adsorbed on the $V_2O_8H_9–NO_3$ cluster, via a transition state (TS1). In TS1, the hydrogen of HNO_3 is being transferred to the hydroxyl oxygen of $V^{4+}–OH$ accompanied by the weakening of the interaction between vanadium and the hydroxyl. Meanwhile, the interaction between the oxygen of HNO_3 and vanadium of $V^{4+}–OH$ is being formed. This process possesses an activation energy of 4.5 kcal/mol and an exothermic energy of 3.96 kcal/mol. The H_2O in the $V_2O_8H_9–NO_3–H_2O$, cluster will desorb from the $V_2O_8H_9–NO_3$ (Fig. 9), since it is endothermic by 6.58 kcal/mol. Afterwards, $V_2O_8H_9–NO_3$ will transform into $V_2O_9H_9$, with the production of NO_2, via a transition state (TS2). In TS2, NO_2 is desorbing from $V_2O_9H_9$, and simultaneously a $V^{5+}=O$ bond is being formed. This NO_2 desorption process, costing an activation energy of 7.44 kcal/mol and finally being exothermic by 41.06 kcal/mol, turns out to be the rate-determining step of the reoxidation reaction. The release of NO_2 from the reoxidation of $V^{4+}–OH$ by HNO_3 has

been confirmed by an experiment carried out by several authors [8,11,12,16].

Frequency calculations were carried out to compare with the experimental results of several publications. In our work, the HNO_3 cluster adsorbed on to $V_2O_9H_{10}$ has a stretching frequency of 1265 cm^{-1}, in good agreement with the 1252 cm^{-1} measured by Miyata and co-workers. Dines et al. [36] reported in 1991 that NO_2 adsorbed on to a V_2O_5 surface would produce a bidentate nitrato ($V^{5+}–NO_3$), which has a $\nu3$ vibration at 1572 cm^{-1}, in accordance with the 1596 cm^{-1} from our calculation for $V_2O_8H_9–NO_3$.

3.2.3. Reaction of the by-product trans-HNO$_2$

One of the products of reaction (7), *trans*-HNO_2, can either react with NH_3 to give H_2NNO and H_2O (Eq. (11)) or another *trans*-HNO_2 to produce NO, NO_2 and H_2O (Eq. (12)). Reactions (11) and (12) were both investigated with DFT calculations. The relative energy profiles are given in Fig. 11.

The reaction between *trans*-HNO_2 and NH_3 on the catalyst surface also has two types, i.e. reaction of adsorbed NH_3 with gaseous *trans*-HNO_2 (D1–D5) and reaction of adsorbed *trans*-HNO_2 with gaseous NH_3 (E1–E5). The reaction between adsorbed NH_3 and gaseous *trans*-HNO_2 starts from the adsorption of NH_3 on to the catalyst surface, which is exothermic by 12.85 kcal/mol. In the transition state D3 (Fig. 11), one hydrogen from the NH_3 is being transferred to the hydroxyl oxygen of *trans*-HNO_2, resulting in the formation of H_2O and H_2NNO (readily transform to N_2 and H_2O [5]). The whole process costs an activation energy of 28.04 kcal/mol and eventually has an exothermic energy of 7.27 kcal/mol:

$$trans\text{-}HNO_2 + NH_3 \rightarrow H_2NNO + H_2O \tag{11}$$
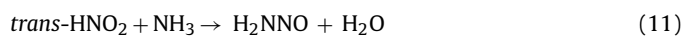
The other type of Eq. (11) is the reaction of adsorbed *trans*-HNO_2 and gaseous NH_3. This reaction possesses an energy barrier of 24.06 kcal/mol, consumed by the transformation of E4–E5, i.e. the desorption of H_2O and H_2NNO from the catalyst surface.

Reaction (12) (Eq. (12)) occurs between two *trans*-HNO_2. In transition state F3, one hydrogen of *trans*-HNO_2 is being transferred to the hydroxyl oxygen of the adsorbed *trans*-HNO_2, costing an activation energy of 5.04 kcal/mol and producing F4 (H_2O, NO and NO_2 adsorbed on the catalyst surface). Afterwards, H_2O, NO and NO_2 will desorb from the catalyst surface, consuming an energy of
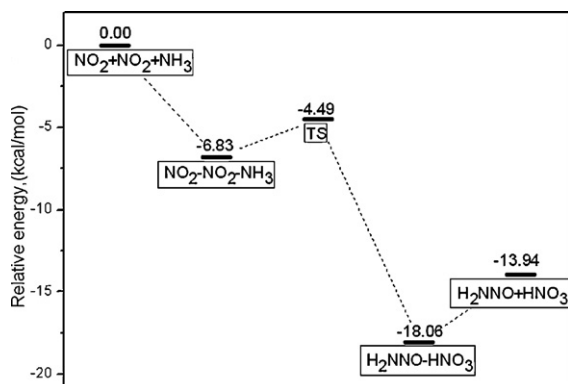

Fig. 8. Energy profile for the reaction between NO_2 and NH_3 (relative to $NO_2 + NO_2 + NH_3$).
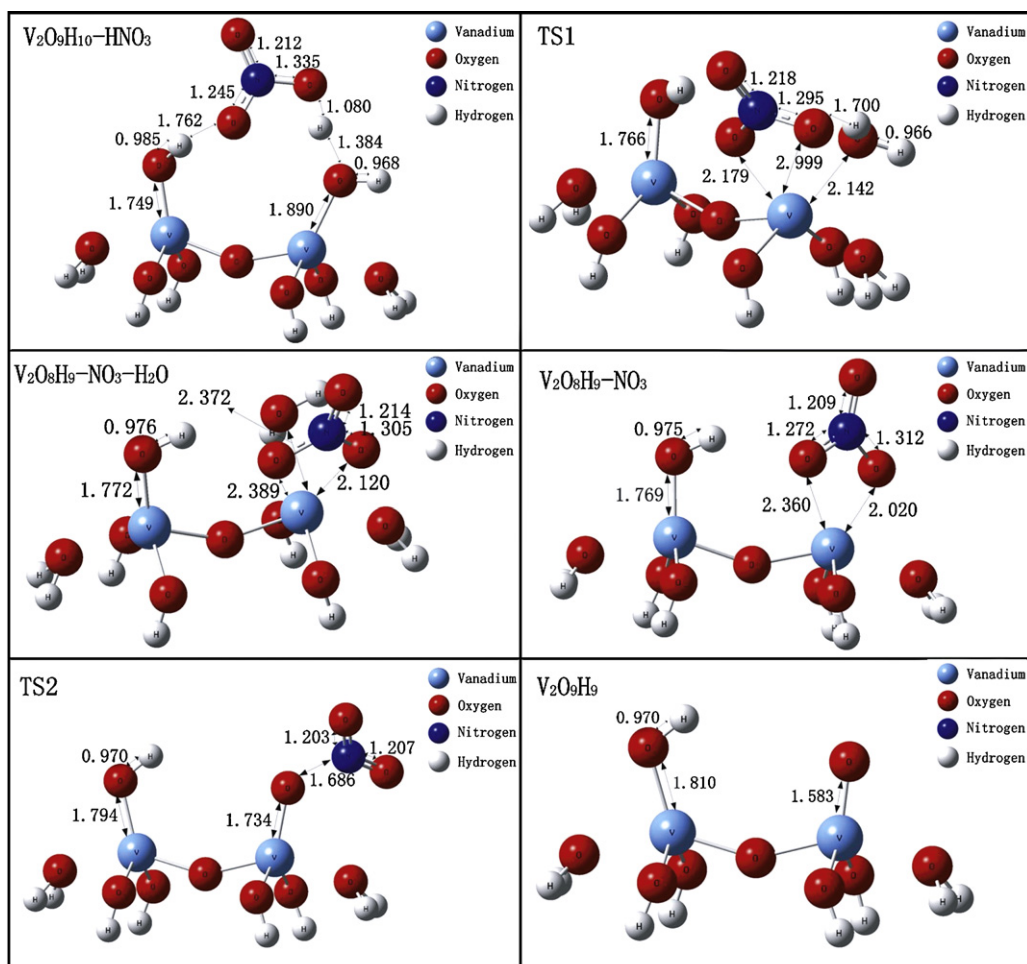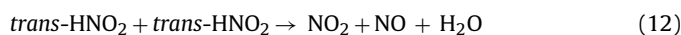
Fig. 9. Optimized structures of all the stationary points in the reoxidization of V^{4+}–OH by HNO_3. Bond lengths are in Å.

24.05 kcal/mol:

$$trans\text{-}HNO_2 + trans\text{-}HNO_2 \rightarrow NO_2 + NO + H_2O \qquad (12)$$

The comparison between reactions (11) (two types) and (12) shows a similar energy profile. The energy barriers of these three reactions are 28.04 kcal/mol (adsorbed NH_3 with gaseous $trans$-HNO_2), 24.06 kcal/mol (adsorbed $trans$-HNO_2 with gaseous NH_3)

and 24.05 kcal/mol (adsorbed $trans$-HNO_2 with gaseous $trans$-HNO_2). Thus, reactions (11) and (12) can equally happen on the catalyst surface.

3.3. Discussion

The first step of the SCR reaction is the reaction of NH_3 and NO on V^{5+}=O, causing a reduction of V^{5+}=O to V^{4+}–OH (Eq. (13)) [3]:

$$V^{5+}\text{=}O + NH_3 + NO \rightarrow V^{4+}\text{--OH} + H_2O + N_2 \qquad (13)$$
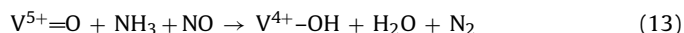
The reduced V^{4+}–OH must be reoxidized in order to participate in the SCR reaction, as revealed by several authors [9,13]. NO_2 can reoxidize V^{4+}–OH via two reaction routes, as discussed in Sections 3.1 and 3.2. Fig. 12 shows the behavior of NO_2 in the reoxidation of V^{4+}–OH to V^{5+}=O. The rate-determining step of route 1 (the direct reoxidation of V^{4+}–OH by NO_2) is the desorption of cis-HNO_2 from $V_2O_9H_9$, with an activation energy of 9.91 kcal/mol. Route 2 (the reoxidation of V^{4+}–OH by HNO_3 produced by the reaction of NO_2 with H_2O or the reaction of NO_2 with NH_3) costs a lower activation energy of 7.44 kcal/mol, as required by the transformation of V^{5+}–NO_3 to V^{5+}=O and NO_2. Accordingly, route 2 is more predominant than route 1 at low temperatures, in accordance with numerous publications [8,11–13,15]; these have proposed that nitrate is much more important for the "fast SCR" at temperatures below 200 °C.

Both routes 1 and 2 will produce nitrous acid (cis-HNO_2 by route 1, $trans$-HNO_2 by route 2). The calculations show that both cis-HNO_2 and $trans$-HNO_2 can either react with NH_3, producing H_2O
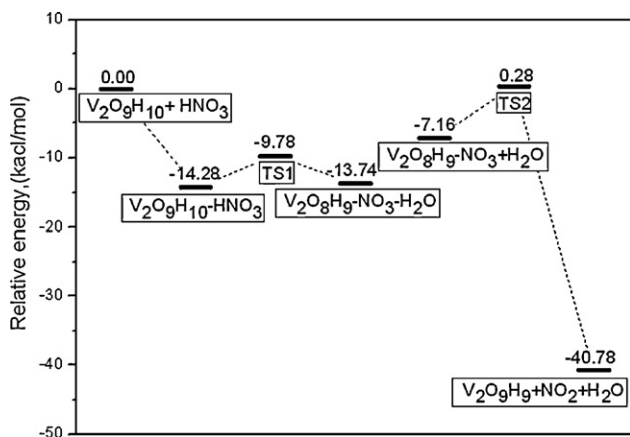

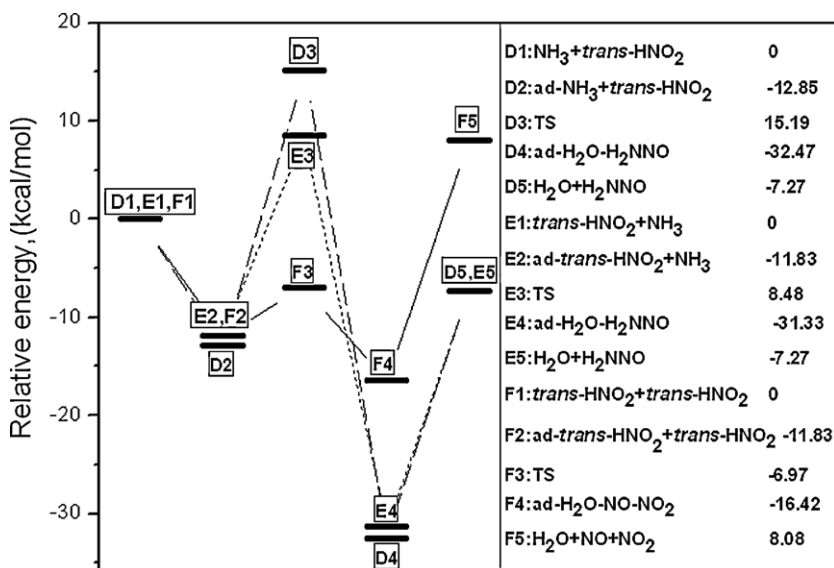**Fig. 10.** Energy profile for the reoxidization of V^{4+}–OH by HNO_3 (relative to $V_2O_9H_{10} + HNO_3$).

Fig. 11. Energy profile for the reaction between adsorbed NH_3 and gaseous trans-HNO_2 (D1–D5, relative to NH_3 + cis-HNO_2); adsorbed trans-HNO_2 and gaseous NH_3 (E1–E5, relative to NH_3 + trans-HNO_2), adsorbed trans-HNO_2 and gaseous trans-HNO_2 (F1–F5, relative to trans-HNO_2 + trans-HNO_2). 'ad-' indicates the adsorbed species on the catalyst surface. The values (given in kcal/mol) on the right side of this figure are the corresponding relative energies.

and N_2, or react with themselves, producing H_2O, NO and NO_2. The energy profile shows that cis-HNO_2 would rather react with itself than react with NH_3. Energy profiles indicated that the reaction between two cis-HNO_2 has an energetic advantage of more than 7.5 kcal/mol than the reaction between cis-HNO_2 and NH_3. Nevertheless, trans-HNO_2 can equally react with itself or with NH_3 on the catalyst surface.

The combination of route 1 (Eq. (4)) and the preferred reaction (Eq. (6)) of its by-product, cis-HNO_2, is given in Eq. (14). This stoichiometry is in close agreement with the experimental results reported by Koebel et al. [9], who found that the reoxidation of the V_2O_5 catalyst follows the reaction given in Eq. (13) in the absence of NH_3. NO will further react with NH_3 over the reoxidized V_2O_5 surface, according to Eq. (13). Therefore, the overall stoichiometry turns out to be the equation of the "fast SCR" (Eq. (2)):
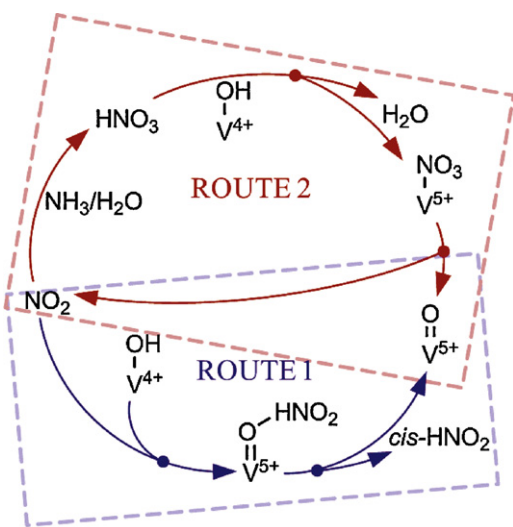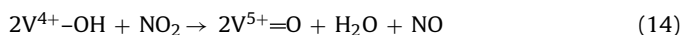
$$2V^{4+}-OH + NO_2 \rightarrow 2V^{5+}=O + H_2O + NO \tag{14}$$

Fig. 12. Reaction routes for the reoxidization of V^{4+}–OH by NO_2. Route 1 represents the direct reoxidization of V^{4+}–OH by NO_2; route 2 represents the reoxidization of V^{4+}–OH by HNO_3 produced by the reaction of NO_2 with H_2O or NH_3.

The overall stoichiometry of route 2, combining the reactions of Eq. (7), 11(12), 9, 10, 13 or 8, 9, 10, 13, is also in accordance with the main reaction of the "fast SCR" (Eq. (2)). The reaction between NH_4NO_3 and NO over V_2O_5 catalyst reported by Koebel et al. [8], Ciardelli et al. [11] and Nova et al. [12] can also be well explained by route 2. Initially, NH_4NO_3 decomposes to NH_3 and HNO_3. Then HNO_3 can readily reoxidize V^{4+}–OH according to Eqs. (9) and (10). Afterwards, the reoxidized V^{5+}=O will be reduced following the reaction of Eq. (13). The overall reaction is given in Eq. (15):

$$NH_4NO_3 + NO \rightarrow NO_2 + N_2 + H_2O \tag{15}$$
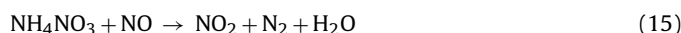
4. Conclusion

DFT calculations have been carried out to study the behavior of NO_2 in the selective catalytic reduction of nitric oxides with ammonia on the V_2O_5 catalyst surface at the B3LYP/6-31G(d,p) level. The results show that NO_2 can readily reoxidize V^{4+}–OH through two reaction routes: (1) NO_2 directly reoxidizes V^{4+}–OH to V^{5+}=O and (2) NO_2 reacts with H_2O or NH_3 to produce HNO_3, which subsequently reoxidizes V^{4+}–OH to V^{5+}=O. For these two reaction channels, we have explored the respective energy profiles and identified the corresponding rate-determining steps. The rate-determining step of route 1 is the desorption of cis-HNO_2 from the reoxidized V^{5+}=O, being endothermic by 9.91 kcal/mol. Route 2 possesses an activation energy of 7.44 kcal/mol (less than route 1), consumed in the desorption of NO_2 from V^{5+}=O. Energetic comparisons show that route 2 is the predominant reaction mechanism at low temperature. Frequency calculations of the species, including V^{5+}=O, V^{4+}–OH, NO_2 adsorbed on V^{4+}–OH, HNO_2 adsorbed on V^{5+}=O and HNO_3 adsorbed on V^{4+}–OH, agree well with previous experimental results carried out by other authors, confirming the rationality of our model cluster.

The reactions of the by-product, HNO_2, were also investigated. The by-product of route 1, cis-HNO_2, can either react with NH_3 or another cis-HNO_2. The reaction of two cis-HNO_2 producing H_2O, NO and NO_2 has an activation energy of 18.40 kcal/mol, while the reaction between cis-HNO_2 and NH_3 possesses a considerably higher energy barrier of 25.99 kcal/mol (reaction of adsorbed cis-HNO_2 with gaseous NH_3). The energy profile for the behavior of trans-HNO_2, the by-product of route 2, shows difference to that for

cis-HNO$_2$. The rate-determining step of the reaction between two *trans*-HNO$_2$ and the reaction between *trans*-HNO$_2$ and NH$_3$ will cost activation energies of 24.05 kcal/mol and 24.06 kcal/mol (reaction of adsorbed *cis*-HNO$_2$ with gaseous NH$_3$), respectively. These results showed that both *cis*-HNO$_2$ (route 1) prefer to reacting with themselves, producing H$_2$O, NO and NO$_2$, rather than reacting with NH$_3$. Nevertheless, *trans*-HNO$_2$ will equally react with itself, producing H$_2$O, NO and NO$_2$ or with NH$_3$, producing H$_2$O and N$_2$ on the catalyst surface. A systematic description of the behavior for NO$_2$ in the "fast" SCR has been proposed in our work, as shown in Fig. 12.

Acknowledgements

References

[1] G. Busca, L. Lietti, G. Ramis, F. Berti, Applied Catalysis B: Environmental 18 (1998) 1–36.
[2] J. Due-Hansen, S. Boghosian, A. Kustov, P. Fristrup, G. Tsilomelekis, K. Stahl, C.H. Christensen, R. Fehrmann, Journal of Catalysis 251 (2007) 459–473.
[3] G. Ramis, G. Busca, F. Bregani, P. Forzatti, Applied Catalysis 64 (1990) 259–278.
[4] N.Y. Topsoe, Science 265 (1994) 1217–1219.
[5] S. Soyer, A. Uzun, S. Senkan, I. Onal, A Quantum Chemical Study of Nitric Oxide Reduction by Ammonia (SCR reaction) on V$_2$O$_5$ Catalyst Surface, Elsevier Science B.V., Hancock, MA, 2005, pp. 268–278.
[6] A. Kato, S. Matsuda, F. Nakajima, M. Imanari, Y. Watanabe, Journal of Physical Chemistry 85 (1981) 1710–1713.
[7] M. Koebel, M. Elsener, G. Madia, Industrial & Engineering Chemistry Research 40 (2001) 52–59.
[8] M. Koebel, G. Madia, M. Elsener, Catalysis Today 73 (2002) 239–247.
[9] M. Koebel, G. Madia, F. Raimondi, A. Wokaun, Journal of Catalysis 209 (2002) 159–165.
[10] G. Madia, M. Koebel, M. Elsener, A. Wokaun, Industrial & Engineering Chemistry Research 41 (2002) 4008–4015.
[11] C. Ciardelli, I. Nova, E. Tronconi, D. Chatterjee, B. Bandl-Konrad, Chemical Communications (2004) 2718–2719.
[12] I. Nova, C. Ciardelli, E. Tronconi, D. Chatterjee, B. Bandl-Konrad, Catalysis Today 114 (2006) 3–12.
[13] E. Tronconi, I. Nova, C. Ciardelli, D. Chatterjee, M. Weibel, Journal of Catalysis 245 (2007) 1–10.
[14] C. Ciardelli, I. Nova, E. Tronconi, D. Chatterjee, B. Bandl-Konrad, M. Weibel, B. Krutzsch, Applied Catalysis B: Environmental 70 (2007) 80–90.
[15] C. Ciardelli, I. Nova, E. Tronconi, D. Chatterjee, T. Burkhardt, M. Weibel, Chemical Engineering Science 62 (2007) 5001–5006.
[16] I. Nova, C. Ciardelli, E. Tronconi, D. Chatterjee, M. Weibel, Topics in Catalysis 42–43 (2007) 43–46.
[17] A. Savara, M.J. Li, W.M.H. Sachtler, E. Weitz, Applied Catalysis B: Environmental 81 (2008) 251–257.
[18] E. Tronconi, I. Nova, C. Ciardelli, D. Chatterjee, B. Bandl-Konrad, T. Burkhardt, Catalysis Today 105 (2005) 529–536.
[19] J.H. Goo, M.F. Irfan, S.D. Kim, S.C. Hong, Chemosphere 67 (2007) 718–723.
[20] C. Ciardelli, I. Nova, E. Tronconi, M. Ascherfeld, W. Fabinski, Topics in Catalysis 42–43 (2007) 161–164.
[21] J. Li, S.H. Li, Journal of Physical Chemistry C 112 (2008) 16938–16944.
[22] M.J. Frisch, G.W. Trucks, H.B. Schlegel, G.E. Scuseria, M.A. Robb, J.R. Cheeseman, J.A. Montgomery Jr., T. Vreven, K.N. Kudin, J.C. Burant, J.M. Millam, S.S. Iyengar, J. Tomasi, V. Barone, B. Mennucci, M. Cossi, G. Scalmani, N. Rega, G.A. Petersson, H. Nakatsuji, M. Hada, M. Ehara, K. Toyota, R. Fukuda, J. Hasegawa, M. Ishida, T. Nakajima, Y. Honda, O. Kitao, H. Nakai, M. Klene, X. Li, J.E. Knox, H.P. Hratchian, J.B. Cross, C. Adamo, J. Jaramillo, R. Gomperts, R.E. Stratmann, O. Yazyev, A.J. Austin, R. Cammi, C. Pomelli, J.W. Ochterski, P.Y. Ayala, K. Morokuma, G.A. Voth, P. Salvador, J.J. Dannenberg, V.G. Zakrzewski, S. Dapprich, A.D. Daniels, M.C. Strain, O. Farkas, D.K. Malick, A.D. Rabuck, K. Raghavachari, J.B. Foresman, J.V. Ortiz, Q. Cui, A.G. Baboul, S. Clifford, J. Cioslowski, B.B. Stefanov, G. Liu, A. Liashenko, P. Piskorz, I. Komaromi, R.L. Martin, D.J. Fox, T. Keith, M.A. Al-Laham, C.Y. Peng, A. Nanayakkara, M. Challacombe, P.M.W. Gill, B. Johnson, W. Chen, M.W. Wong, C. Gonzalez, J.A. Pople, Gaussian 03, Revision B. 02, Gaussian Inc., Pittsburgh PA, 2003.
[23] A.D. Becke, Journal of Chemical Physics 98 (1993) 5648–5652.
[24] A.D. Becke, Physical Review A 38 (1988) 3098–3100.
[25] C.T. Lee, W.T. Yang, R.G. Parr, Physical Review B 37 (1988) 785–789.
[26] M.D. Halls, J. Velkovski, H.B. Schlegel, Theoretical Chemistry Accounts 105 (2001) 413–421.
[27] A. Gora, E. Broclawik, Journal of Molecular Catalysis A: Chemical 215 (2004) 187–193.
[28] E. Broclawik, A. Gora, M. Najbar, The Role of Tungsten in Formation of Active Sites for no SCR on the V–W–O Catalyst Surface—Quantum Chemical Modeling (DFT), Elsevier Science B.V., Leuven, Belgium, 1999, pp. 31–38.
[29] A. Gora, E. Broclawik, M. Najbar, Quantum Chemical Modeling (DFT) of Active Species on the V–W–O Catalyst Surface in Various Redox Conditions, Pergamon–Elsevier Science Ltd., Szklarska, Poland, 1999, pp. 405–410.
[30] N.A. Kachurovskaya, E.P. Mikheeva, G.M. Zhidomirov, Journal of Molecular Catalysis A: Chemical 178 (2002) 191–198.
[31] M. Witko, K. Hermann, R. Tokarz, Adsorption and Reactions at the (0 1 0) V$_2$O$_5$ Surface: Cluster Model Studies, Elsevier Science B.V., San Francisco, CA, 1999, pp. 553–565.
[32] M. Calatayud, B. Mguig, C. Minot, Surface Science 526 (2003) 297–308.
[33] M. Calatayud, F. Tielens, F. De Proft, Chemical Physics Letters 456 (2008) 59–63.
[34] M. Calatayud, C. Minot, Reactivity of the V$_2$O$_5$–TiO$_2$-Anatase Catalyst: Role of the Oxygen Sites, Springer/Plenum Publishers, Philadelphia, PA, 2004, pp. 17–26.
[35] A. Michalak, M. Witko, K. Hermann, Surface Science 375 (1997) 385–394.
[36] T.J. Dines, C.H. Rochester, A.M. Ward, Journal of the Chemical Society, Faraday Transactions 87 (1991) 1617–1622.
[37] H. Miyata, S. Konishi, T. Ohno, F. Hatayama, Journal of the Chemical Society, Faraday Transactions 91 (1995) 1557–1562.
[38] A.M. Mebel, M.C. Lin, C.F. Melius, Journal of Physical Chemistry A 102 (1998) 1803–1807.